Error Budgets: A Path from Uncertainty Quantification to Model Validation

Roger Ghanem

Aerospace and Mechanical Engineering
Civil Engineering
University of Southern California
Los Angeles

Advanced Simulation and Computing Workshop: Error Estimation, Uncertainty Quantification, and Reliability in Numerical Simulations, Aug 22nd 23rd, 2005, Stanford, CA.

Acknowledgments

Funding from:

Sandia, ONR, AFOSR, NSF, DARPA, Taisei, Shimizu, ARAMCO

Intellectual contributions:

Graduate students at Buffalo, Hopkins and USC

John Red-Horse - SNL

Habib Najm - SNL

Bert Debusschere - SNL

Christian Soize - UMLV, France

OUTLINE

- Motivation
- Mathematical structure for validation and verification
- Packaging of information using this structure
- Construction of approximation spaces on these structures
- Examples
- Technical challenges and conclusions

A simple prelude

- Quantity of interest: decision with upper bound on risk
  - Flip coin 100 times ⇒ calibrated decision tool ⇒ 50-50
  - ⊕ observe initial configuration ⇒ calibrated decision tool ⇒ 70-30
  - ⊕ observe surface tension ⇒ calibrated decision tool ⇒ 80-20

    --- --- ---

  - ⊕ observe quantum states ⇒ calibrated decision tool ⇒ 99-1
- Use Model-Based Predictions in lieu of physical experiments

Ingredients:

- calibrate a stochastic plant
- evaluate limit on predictability of plant
- refine plant if target confidence not achievable

Interaction of model and data

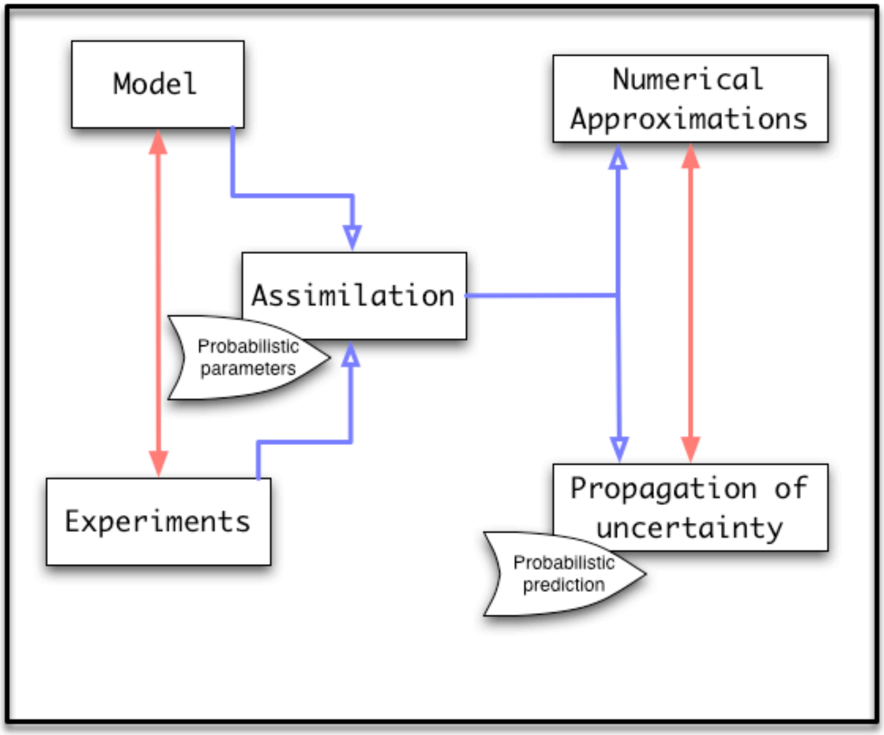

Interaction of model and data

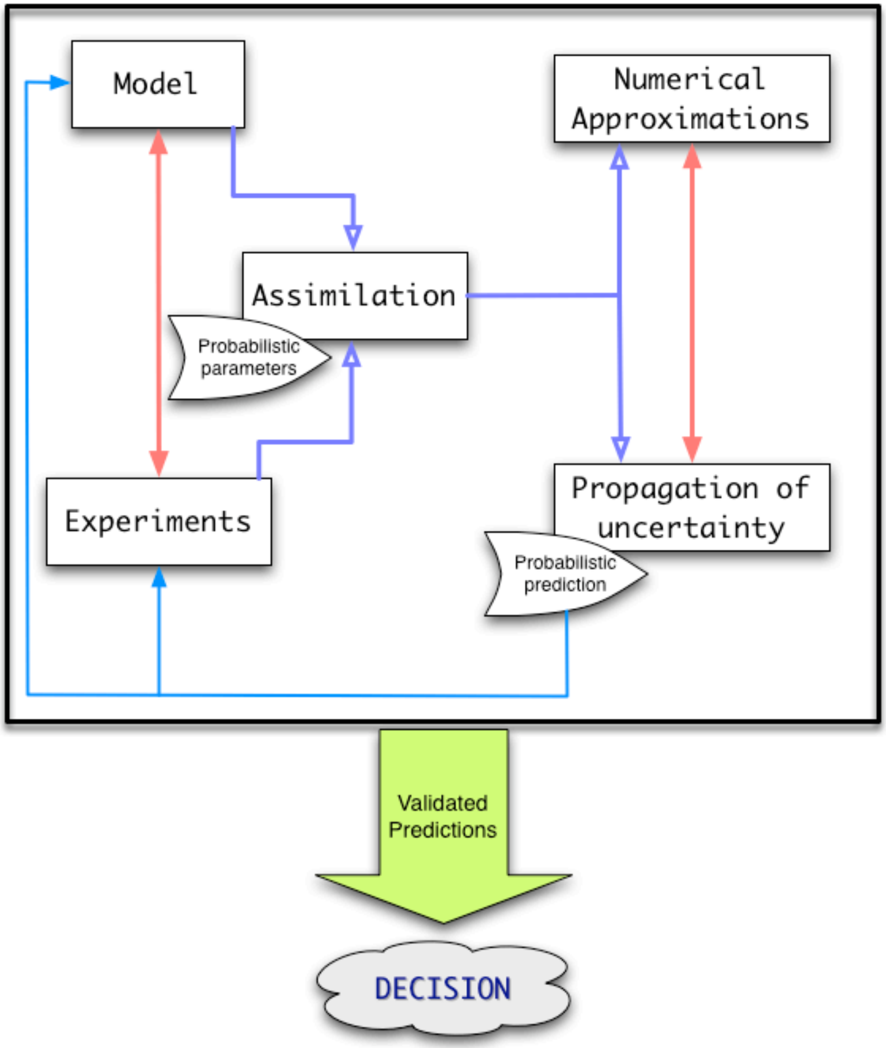

Interaction of model and data

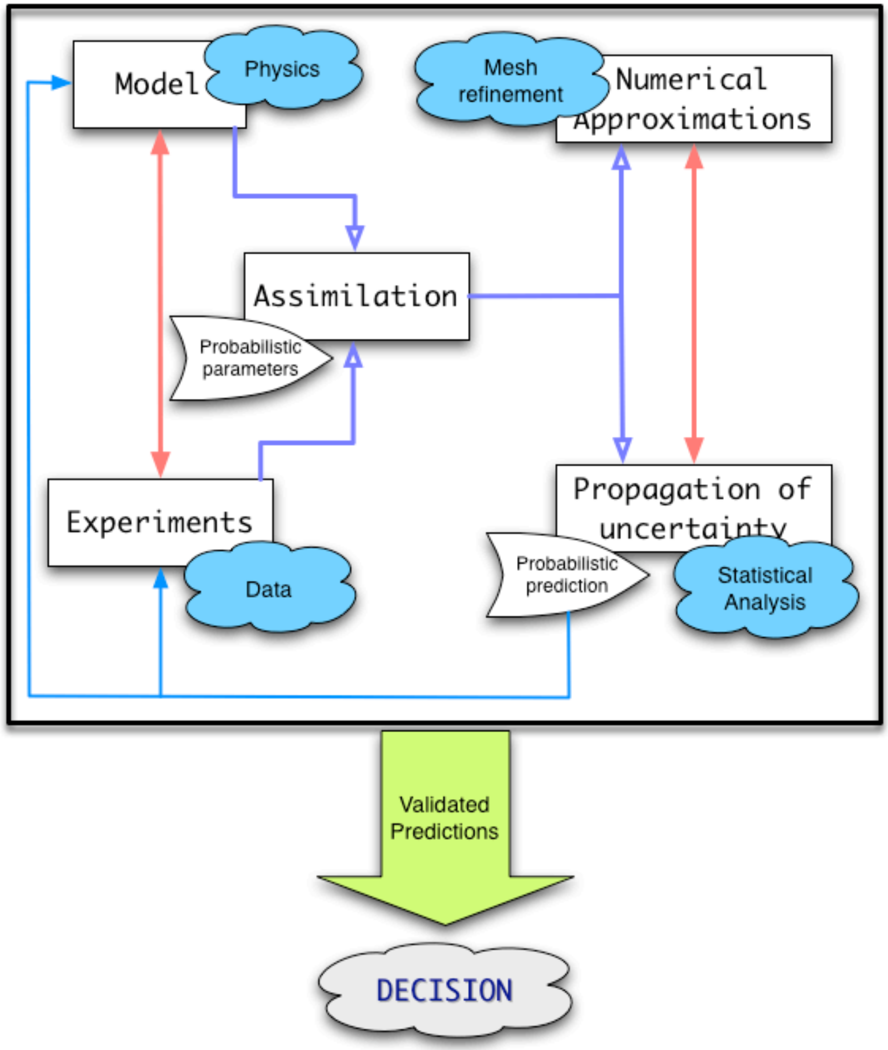

Interaction of model and data

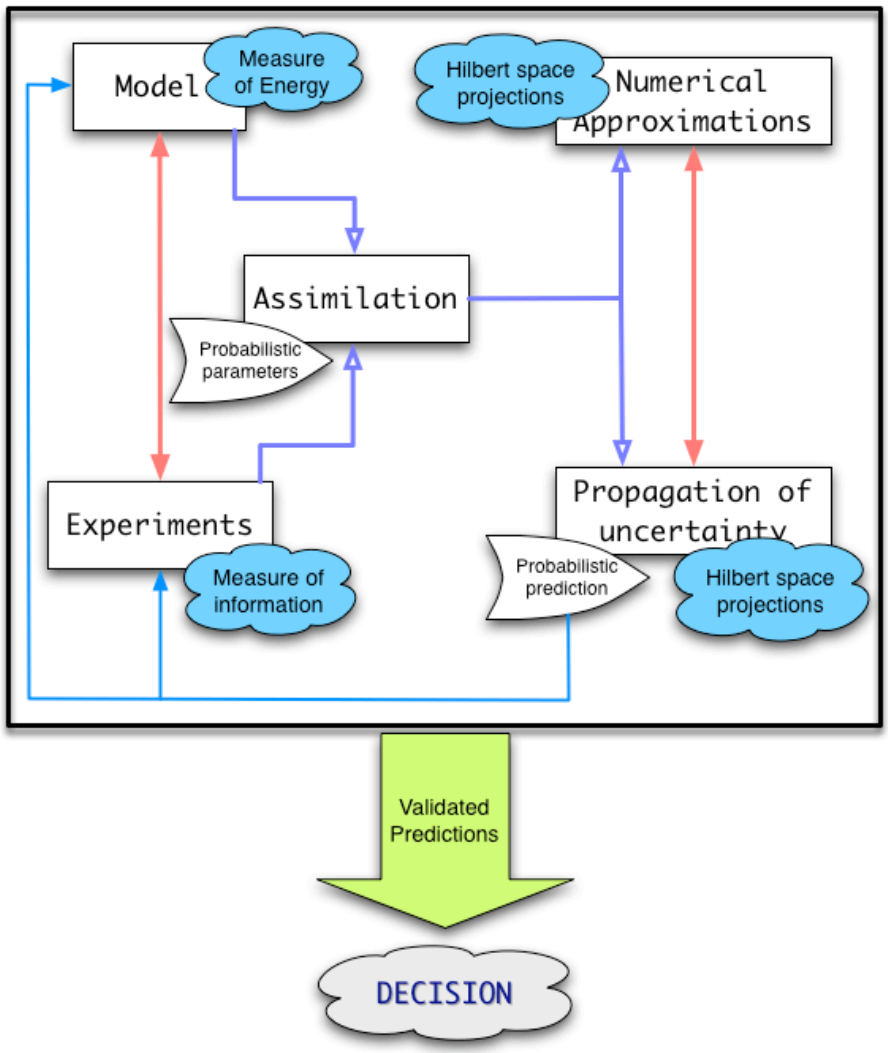

Interaction of model and data

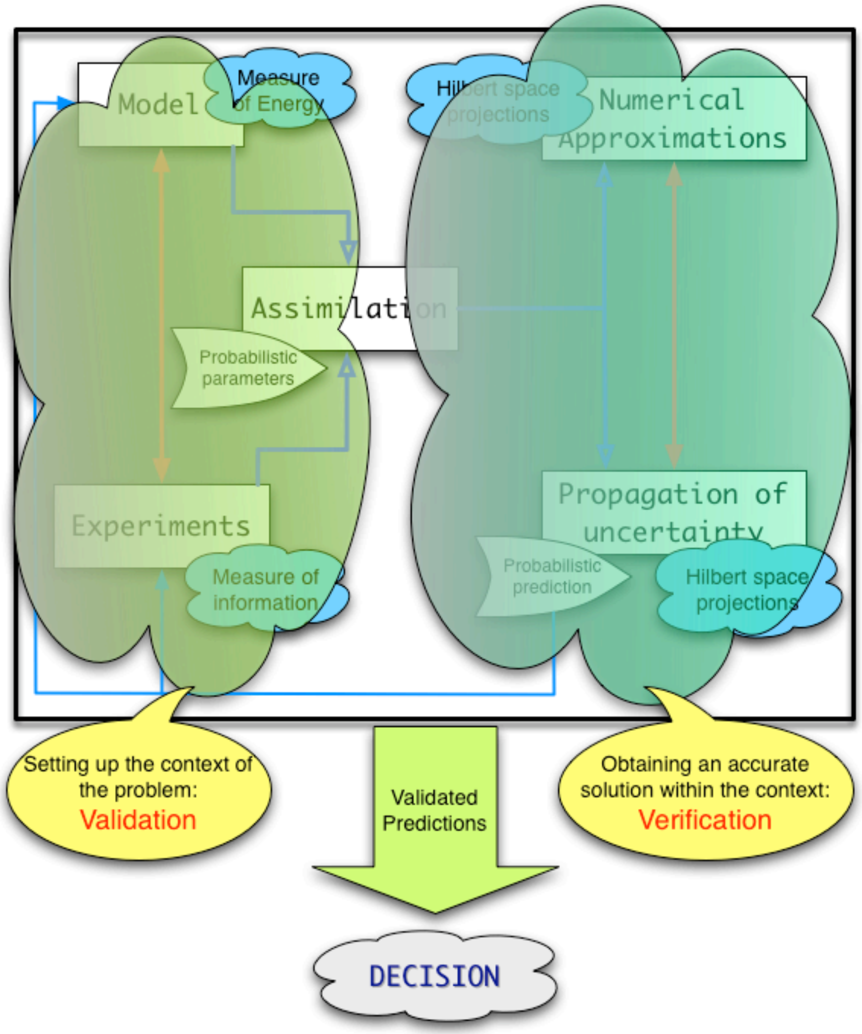

Error budget

$$\mathbf{U} = \hat{\mathbf{U}}|_{h,d,p,m} + \epsilon_h|_{p,d,m} + \epsilon_p|_{d,m} + \epsilon_d|_m + \epsilon_m$$

$\epsilon_h|_{\mathrm{d,m}}$: can be reduced through better numerics.

$\epsilon_p|_{\mathrm{d,m}}$: can be reduced through better statistics.

$\epsilon_d|_{\mathrm{m}}$: can be reduced through better data.

ϵ_m: can be reduced through better models.

We use probabilistic models for uncertainty

The probabilistic framework provides a packaging of information that is amenable to a level of rigor in analysis that permits the "quantification" of uncertainty.

Although:

"… unacquainted with problems where wrong results could be attributed to failure to use measure theory…." (E.T. Jaynes, published 2003)

An experiment is defined by a probability triple, (a measurable space) $(\mathcal{A}, \mathcal{T}, \mu)$

$\mathcal{A}$	Set of elementary events
$\mathcal{T}$	Sigma algebra of all events that make sense
μ	Measure on all elements of $\mathcal{T}$

A random variable X is a measurable mapping on a probability space $(\mathcal{A}, \mathcal{T}, \mu)$ to $(R, \mathcal{B})$

The probability distribution P of X is the image of μ under X, defining the probability triple $(R, \mathcal{B}, P)$

What do we mean by things being close ?

Modes of Convergence: Let X_n be a sequence of r.v. defined on $(\mathcal{A}, \mathcal{T}, \mu)$ and let Y be another rv on same probability space:

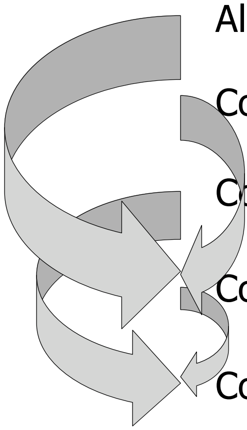

Almost sure Convergence: $P[|X_n - Y| > \epsilon] \rightarrow 0 \quad \forall \epsilon$ $\qquad X_n(\omega)$ converges a.e. to $Y(\omega)$.

Convergence in mean square: $\|X_n - Y\|_{L^2} \rightarrow 0$

Convergence in mean: $\|X_n - Y\|_{L^1} \rightarrow 0$

Convergence in probability: $P[\rho(X_n, Y) < \varepsilon] \rightarrow 1 \quad \forall \varepsilon$

Convergence in distribution: Let $X_n \in L^0(\mathcal{A}_n, \mathcal{T}_n, \mu_n)$ and $Y \in L^0(\mathcal{A}, \mathcal{T}, \mu)$

then X converges in distribution to Y if P_n converges to P

Convergence in mean-square permits an L_2 analysis of random variables.

First step in a unified perspective in verification and validation.

Functional representations

Characterize **Y**, given characterization of $Z^1, \cdots, Z^P$

$$\boldsymbol{Y} = \widetilde{\boldsymbol{f}}(\boldsymbol{Z}^1, \ldots, \boldsymbol{Z}^p)$$

Each Z^j is a vector-valued random variable:

$$\boldsymbol{Z}^j : \quad (\mathcal{A}, \mathcal{T}, P) \longrightarrow \mathbb{R}^{m_j}$$

Orthogonalizing the random variables:

$$\boldsymbol{C}_{\boldsymbol{Z}^j} = \boldsymbol{L}^T_{\boldsymbol{Z}^j} \boldsymbol{L}_{\boldsymbol{Z}^j}$$

$$\boldsymbol{Z}^j = \boldsymbol{m}_{Z^j} + \boldsymbol{L}^T_{Z^j} \boldsymbol{X}^j$$

Then:

$$\boldsymbol{y} = \boldsymbol{f}(\boldsymbol{x}^1, \ldots, \boldsymbol{x}^p) : \quad \mathbb{R}^{m_1} \times \ldots \times \mathbb{R}^{m_p} \rightarrow \mathbb{R}^m$$

Functional representations

Assumptions:

- Second-order random variables:

$$E\left\{\|\boldsymbol{f}(\boldsymbol{X}^1,\ldots,\boldsymbol{X}^p)\|^2\right\} < +\infty$$

- Basic random vectors are independent:

$$P_{\boldsymbol{X}^1,\ldots,\boldsymbol{X}^p} = P_{\boldsymbol{X}^1} \otimes \ldots \otimes P_{\boldsymbol{X}^p}$$

- Vector X^j does not necessarily involve independent random variables:

$$P_{X^j} \neq \prod_{k=1}^{P} P_{X_k^j}$$

Functional representations

$$
\begin{aligned}
\mathbb{H}^{(m)} &= L^2_{P_{\boldsymbol{x}^1,\ldots,\boldsymbol{x}^p}}\left(\mathbb{R}^{m_1} \times \ldots \times \mathbb{R}^{m_p}, \mathbb{C}^m\right) \\
&\simeq \left(L^2_{P_{\boldsymbol{x}^1,\ldots,\boldsymbol{x}^p}}\left(\mathbb{R}^{m_1} \times \ldots \times \mathbb{R}^{m_p}, \mathbb{R}\right)\right) \otimes \mathbb{C}^m \\
&= \left(\otimes_{j=1}^{p} \mathbb{H}_j\right) \otimes \mathbb{C}^m \\
&= \mathbb{H} \otimes \mathbb{C}^m
\end{aligned}
$$

$$
\begin{aligned}
\mathbb{H}_{j,k} &= L^2_{P_{X^j_k}}(\mathbb{R}, \mathbb{R}) \\
\mathbb{H}_j &= \otimes_{k=1}^{m_j} \mathbb{H}_{j,k}
\end{aligned}
$$

Given bases of $H_{j,k}$ other bases can be constructed.

Functional representations

For all $\boldsymbol{x}^j = (x_1^j, \ldots, x_{m_j}^j)$ belonging to the support S_{m_j} of $p_{\boldsymbol{X}^j}(\boldsymbol{x}^j)$, Hilbertian basis $\left\{\phi_{\boldsymbol{\alpha}^j}^j, \quad \boldsymbol{\alpha}^j \in \mathbb{N}^{m_j}\right\}$ of real Hilbert space $\mathbb{H}_j$ is given by

$$\phi_{\boldsymbol{\alpha}^j}^j(\boldsymbol{x}^j) = \left(\frac{p_{X_1^j}(x_1^j) \times \ldots \times p_{X_{m_j}^j}(x_{m_j}^j)}{p_{\boldsymbol{X}^j}(\boldsymbol{x}^j)}\right)^{1/2} \psi_{\alpha_1^j}^1(x_1^j) \times \ldots \times \psi_{\alpha_{m_j}^j}^{m_j}(x_{m_j}^j) \ ,$$

where $\{\psi_{\alpha_k^j}^k(x_k^j)\}_{\alpha_k^j}$ is a Hilbertian basis of real Hilbert space $\mathbb{H}_{j,k}$ and $\boldsymbol{\alpha}^j = (\alpha_1^j, \ldots, \alpha_{m_j}^j)$.

Some common bases

Infinite-dimensional case:
This is an exercise in stochastic analysis:

- Hermite polynomials: Gaussian measure (Wiener: Homogeneous Chaos)
- Charlier polynomials: Poisson measure (Wiener: Discrete Chaos)
- Very few extensions possible: Friedrichs and Shapiro (Integration of functionals) provide characterization of compatible measures. Segall and Kailath provide an extension to martingales.

Finite-dimensional case: independent variables:
This is an exercise in one-dimensional approximation:

- Askey polynomials:measures from Askey chart (Karniadakis and co-workers)
- Legendre polynomials: uniform measure (theoretical results by Babuska and co-workers)
- Wavelets: Le-Maitre and co-workers
- Arbitrary measures with bounded support: C. Schwab

Finite-dimensional case: dependent variables:
This is an exercise in multi-dimensional approximation:

- Arbitrary measures: Soize and Ghanem.

Another special basis: Karhunen-Loeve expansion

A zero-mean stochastic process

$$\lim_{N\to\infty} E \left\| \boldsymbol{U}(\boldsymbol{x},\theta) - \sum_{i=1}^{N} \xi_i(\theta)\sqrt{\lambda_i}\phi_i(\boldsymbol{x}) \right\|_{L_2} = 0 \qquad \mu = \sum_{i=1}^{\infty} \lambda_i < \infty$$

$$\xi_i(\theta) = \frac{1}{\lambda_i}(U,\phi_i)$$

where

$$\boldsymbol{R}_U \boldsymbol{v} = \lambda \boldsymbol{v},$$

is the eigen-problem associated with the covariance function of the process $\boldsymbol{U}(\boldsymbol{x},\theta)$.

The Karhunen-Loeve expansion:

$$\boldsymbol{U}(\boldsymbol{x},\theta) = \sum_{i=1}^{N} \xi_i(\theta)\sqrt{\lambda_i}\phi_i(\boldsymbol{x}) = \sum_{i=1}^{N} (U,\phi_i)_K \phi_i(x) = \sum_{i=1}^{N} (U,\xi_i)\,\xi_i(\theta)$$

If the covariance kernel of $\boldsymbol{U}$ has $2r$ continuous symmetric derivative and is α-Lipschitz, then

$$\lambda_n = O\left(\frac{1}{n^{2r+1+\alpha}}\right)$$

Reference: J.B. Read (1983)

Management of uncertainty

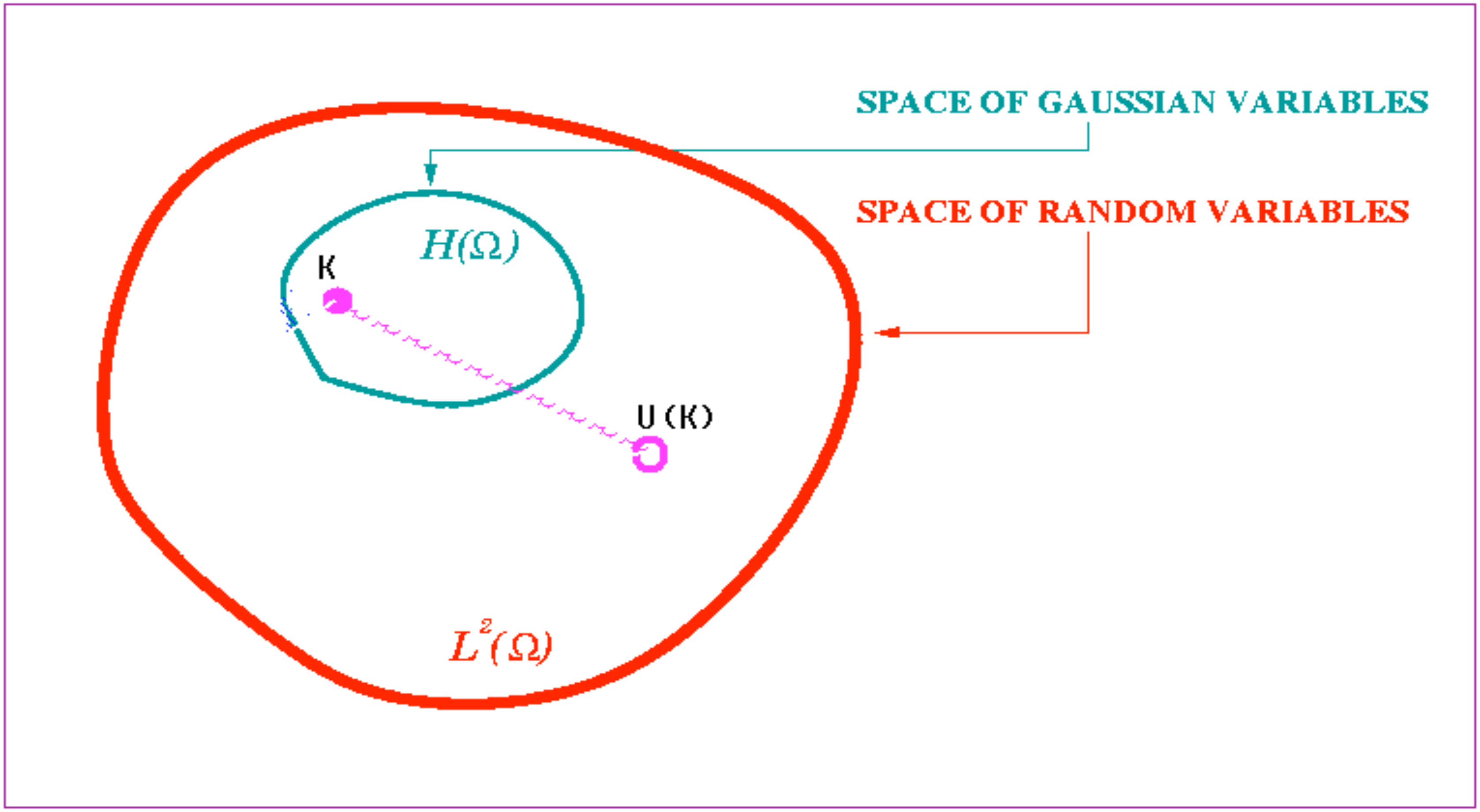

Management of uncertainty

COORDINATES IN THIS SPACE REPRESENT PROBABILISTIC CONTENT.

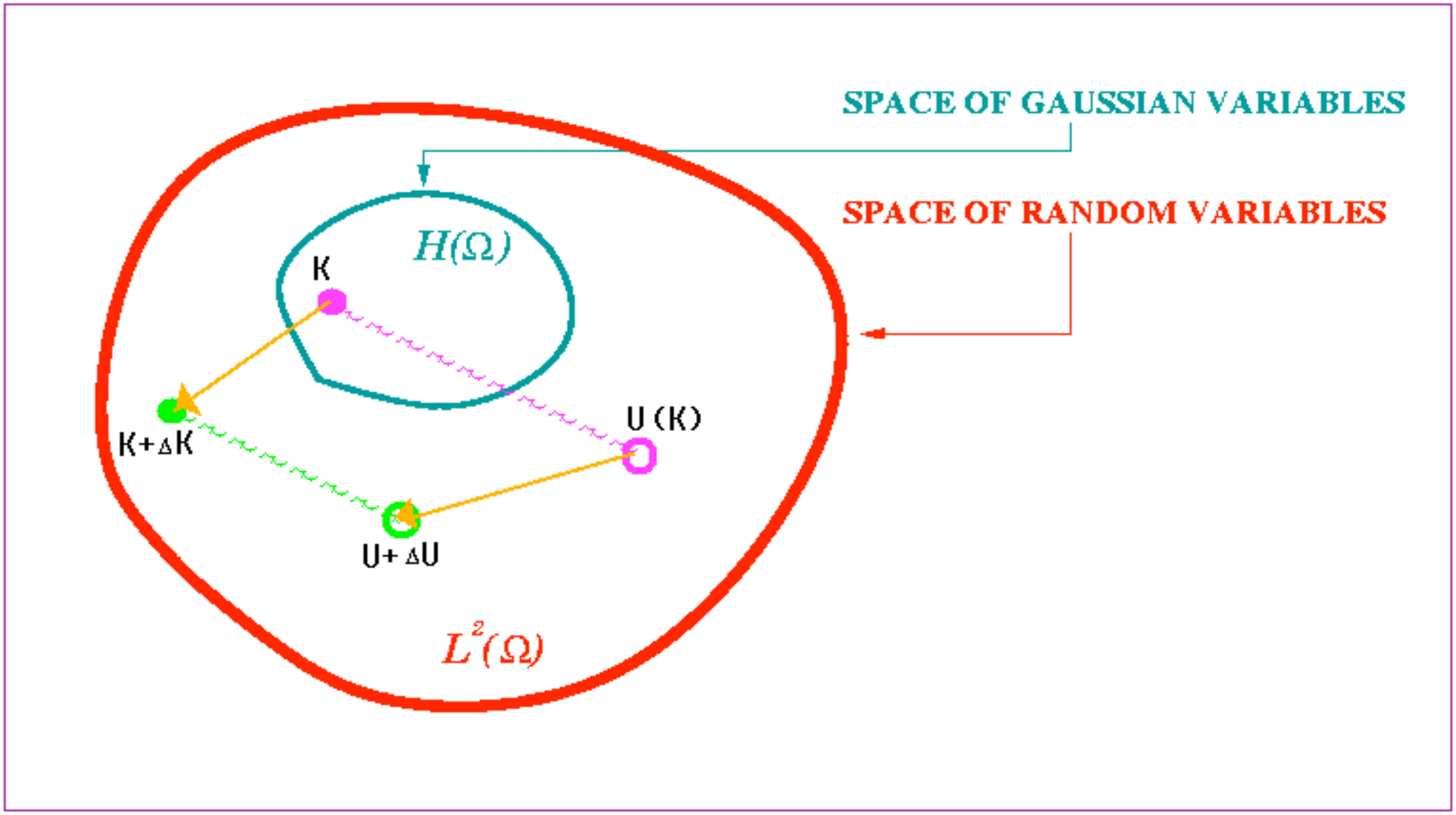

SENSITIVITY OF PROBABILISTIC STATEMENTS OF BEHAVIOR ON DATA.

Representing uncertainty

$$
\begin{aligned}
\psi_0 &= 1 \\
\psi_1 &= \xi_1 \\
\psi_2 &= \xi_2 \\
\psi_3 &= \xi_1^2 - 1 \\
\psi_4 &= \xi_1\xi_2 \\
\psi_5 &= \xi_2^2 - 1 \\
\ldots
\end{aligned}
$$

The random quantities are resolved as

$$\alpha(\mathbf{x},\theta) = \sum_{i=1}^{\infty} \alpha_i(\mathbf{x}) \underbrace{\Psi_i(\{\boldsymbol{\xi}(\theta)\})}$$

Multidimensional Orthogonal Polynomials in independent random variables

These could be, for example:

- Parameters in a PDE
- Boundaries in a PDE (e.g. Geometry)
- Field Variable in a PDE

Arbitrary measures:

Karniadakis

Babuska

LeMaitre/Ghanem

Soize/Ghanem

Representation of uncertainty: Galerkin projection

The random quantities are resolved as

$$\alpha(\mathbf{x},\theta) = \sum_{i=1}^{\infty} \alpha_i(\mathbf{x})\Psi_i(\theta) \qquad \alpha_i(x) = \frac{(\alpha(x,\theta),\psi_i(\theta))_{L_2(\Omega)}}{\|\psi_i(\theta)\|^2_{L_2(\Omega)}}$$

These could be, for example:

- Parameters in a PDE
- Boundaries in a PDE (e.g. Geometry)
- Field Variable in a PDE

These decompositions provide a resolution (or parameterization) of the uncertainty on spatial or temporal scales

Representation of uncertainty: Maximum likelihood

The random quantities are resolved as:

$$\alpha(\mathbf{x},\theta) = \sum_{|i|\le q} \alpha_i(\mathbf{x})\Psi_i(\theta) \qquad KL : \boldsymbol{\eta}_i(\boldsymbol{\theta}) = \frac{1}{\sqrt{\boldsymbol{\lambda}_i}}(\boldsymbol{\alpha}(.,\boldsymbol{\theta}),\boldsymbol{\phi}_i)_{\boldsymbol{H}}$$

Let

$$\boldsymbol{A} = \{\alpha_i(x), \quad |i| \le q\}$$

Likelihood Function is:

$$\begin{aligned}
L(\alpha^1,\ldots,\alpha^M;\boldsymbol{A}) &= p_{\alpha_1(x),\ldots,\alpha_M(x)}(\alpha^1,\ldots,\alpha^m;\boldsymbol{A}) \times \ldots \times p_{\alpha_1(x),\ldots,\alpha_M(x)}(\alpha^1,\ldots,\alpha^M;\boldsymbol{A}) \\
L(\eta^1,\ldots,\eta^m;\boldsymbol{A}) &= p_{\eta_1,\ldots,\eta_m}(\eta^1,\ldots,\eta^m;\boldsymbol{A}) \times \ldots \times p_{\eta_1,\ldots,\eta_m}(\eta^1,\ldots,\eta^m;\boldsymbol{A}) \\
&\approx \prod_{j=1}^{\nu} p_{\eta_j}(\eta_j^1;\boldsymbol{A}) \times \ldots \times \prod_{j=1}^{\nu} p_{\eta_j}(\eta_j^m;\boldsymbol{A})
\end{aligned}$$

Maximum Likelihood:

$$\max_{\boldsymbol{A}} L$$

“essential” dimensionality of a process

Physical object:
Linear Elasticity

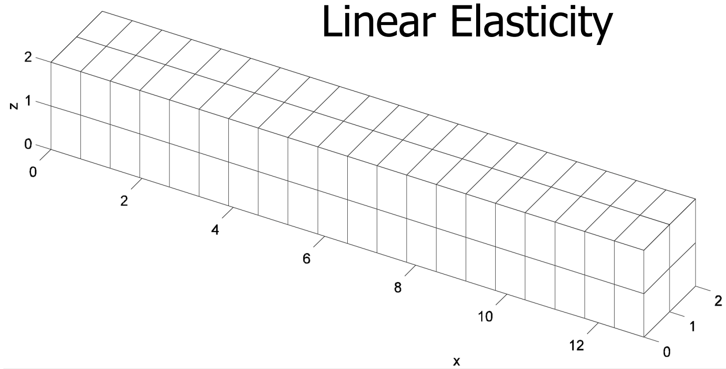

Convergence as function of
“dimensionality”

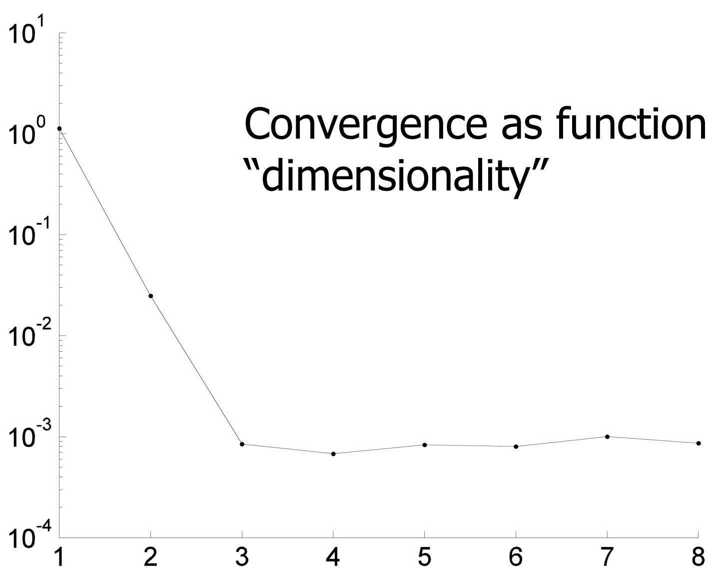

Stochastic parameters

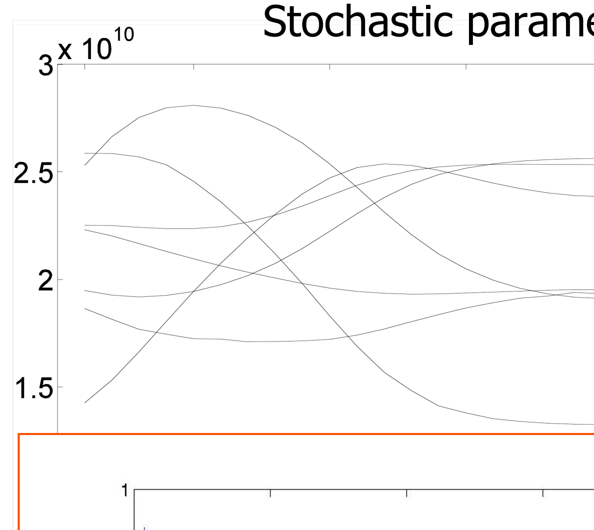

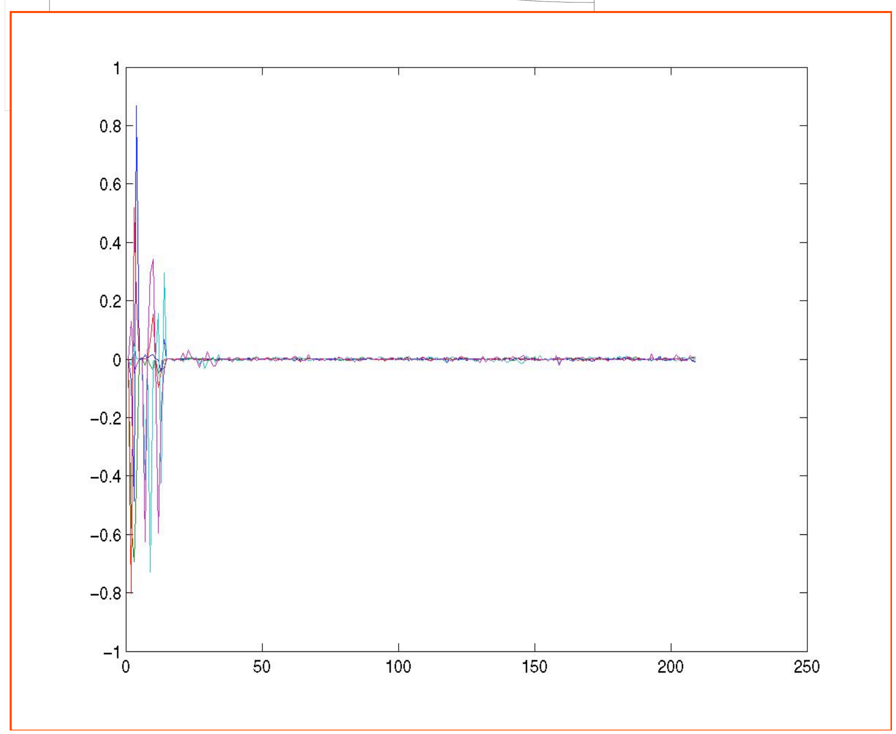

Representation of uncertainty: Bayesian inference

Covariance matrix of observations

$$\hat{C} = \frac{1}{M-1}\sum_{i=1}^{M}(a_i - \bar{a})^T(a_i - \bar{a})$$

Reduced order representation: KL:

$$a(\omega) \approx \bar{a} + \sum_{i=1}^{\mu}\sqrt{\lambda_i}\eta^{(i)}(\omega)\phi_i$$

Where:

$$\begin{cases} \eta_j^{(i)} = \frac{1}{\sqrt{\lambda_i}}\langle a_j, \phi_i\rangle_{l_2} \\ E[\eta^{(n)}] = 0 \quad n, m = 1, \ldots, \mu. \\ E[\eta^{(m)}\eta^{(n)}] = \delta_{mn} \end{cases}$$

Starting with observations of process over a limited subset of indexing set:

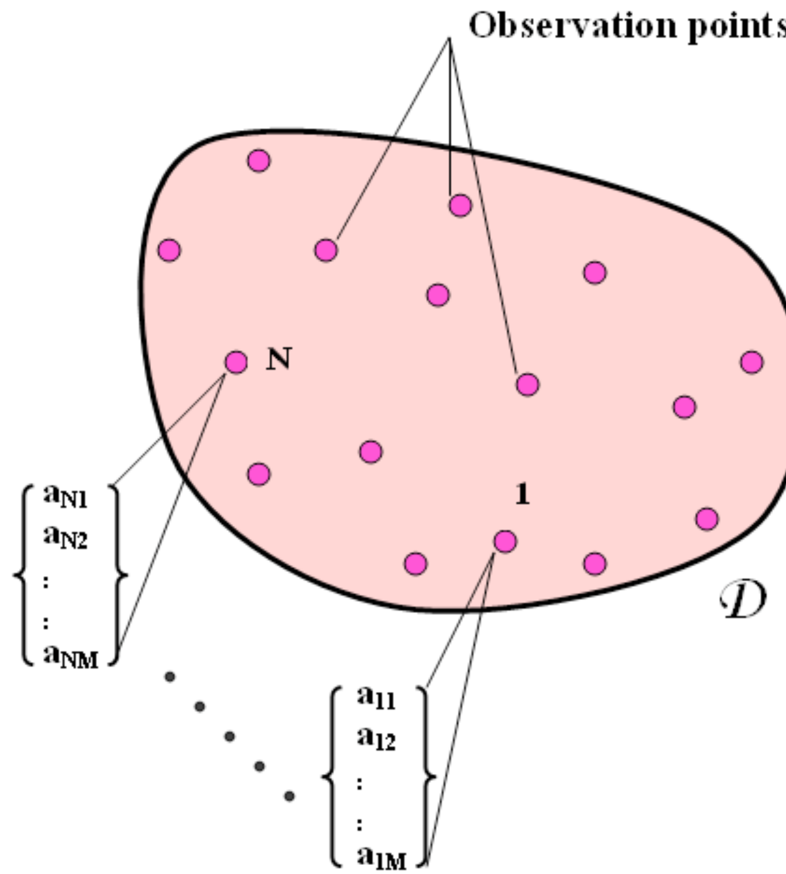

Representation of uncertainty: Bayesian inference

Objective is to estimate $\{\eta_i(\theta)\}$

Polynomial Chaos representation of reduced variables:

$$\hat{\eta}^{(i)} = \sum_{j=1}^{\infty} \gamma_j^{(i)} \bar{\Psi}_j(\xi_i) \approx \sum_{j=1}^{p} \gamma_j^{(i)} \bar{\Psi}_j(\xi_i) \quad i = 1, \ldots, \mu$$

Constraint on chaos coefficients:

$$\sum_{j=1}^{p} (\gamma_j^{(i)})^2 = 1 \quad i = 1, \ldots, \mu.$$

Estimation of stochastic process using estimate of reduced variables:

$$\hat{a}(\omega) = \bar{a} + \sum_{i=1}^{\mu} \sqrt{\lambda_i} \hat{\eta}^{(i)}(\omega) \phi_i.$$

Representation of uncertainty: Bayesian inference

Define Cost Function (hats denote estimators):

$$L[\gamma,\hat{\gamma}] = \begin{cases} 1 & \text{if } \max_{1\le i\le p} |\gamma_i^{(k)} - \hat{\gamma}_i^{(k)}| > \Delta \\ 0 & \text{if } \max_{1\le i\le p} |\gamma_i^{(k)} - \hat{\gamma}_i^{(k)}| \le \Delta, \end{cases}$$

Then Bayes estimate is:

$$\hat{\gamma} = \arg\min_{\zeta} E\{L[\gamma, \zeta(\hat{\eta}_1^{(k)}, \ldots, \hat{\eta}_M^{(k)})]\}$$

$$\approx \arg\min_{\zeta} E\{L[\gamma, \zeta(\eta_1^{(k)}, \ldots, \eta_M^{(k)})]\}.$$

Bayes rule: $\pi[\gamma|\eta_1^{(k)},\ldots,\eta_M^{(k)}] \propto p_{\hat{\eta}^{(k)}}(\eta_1^{(k)},\ldots,\eta_M^{(k)}|\gamma) \times \pi(\gamma)$

- Use kernel density estimation to represent the Likelihood function
- Use Markov Chain Monte Carlo to sample from the posterior (metropolis Hastings algorithm) -->BIMH

Representation of uncertainty: Bayesian inference

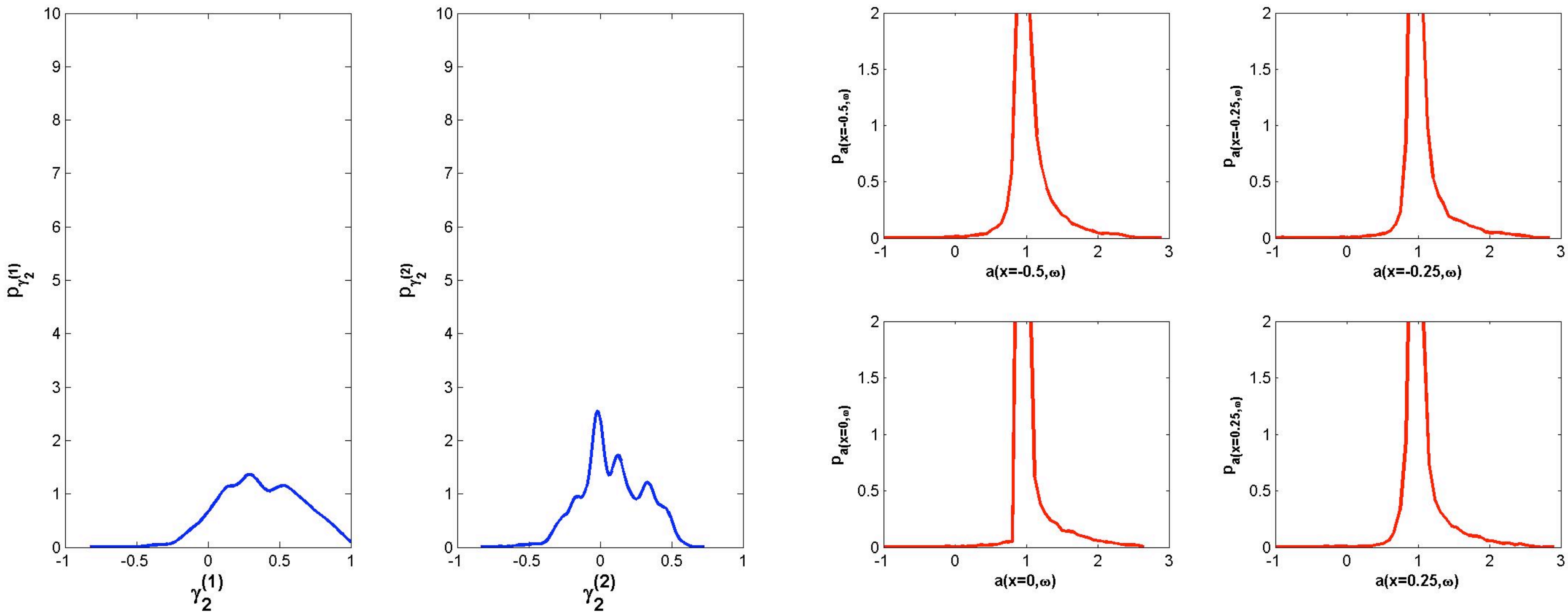

Representation of uncertainty: Bayesian inference

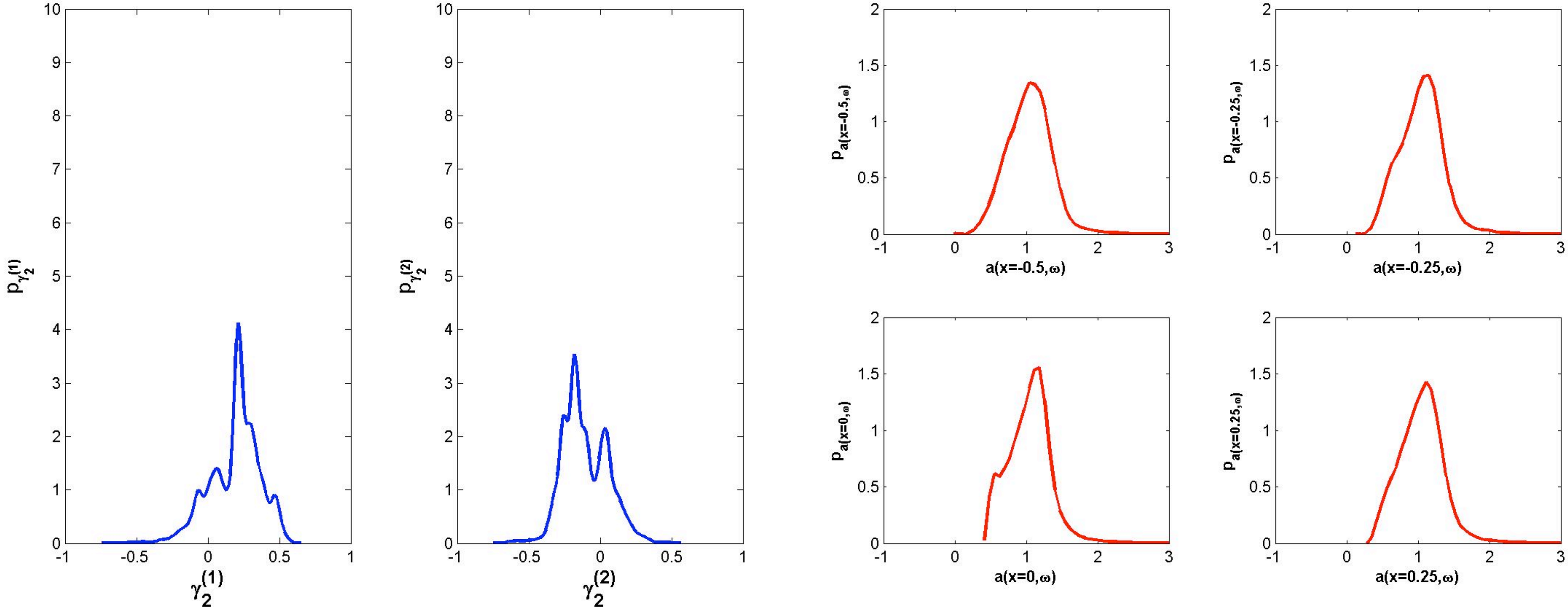

Representation of uncertainty: Bayesian inference

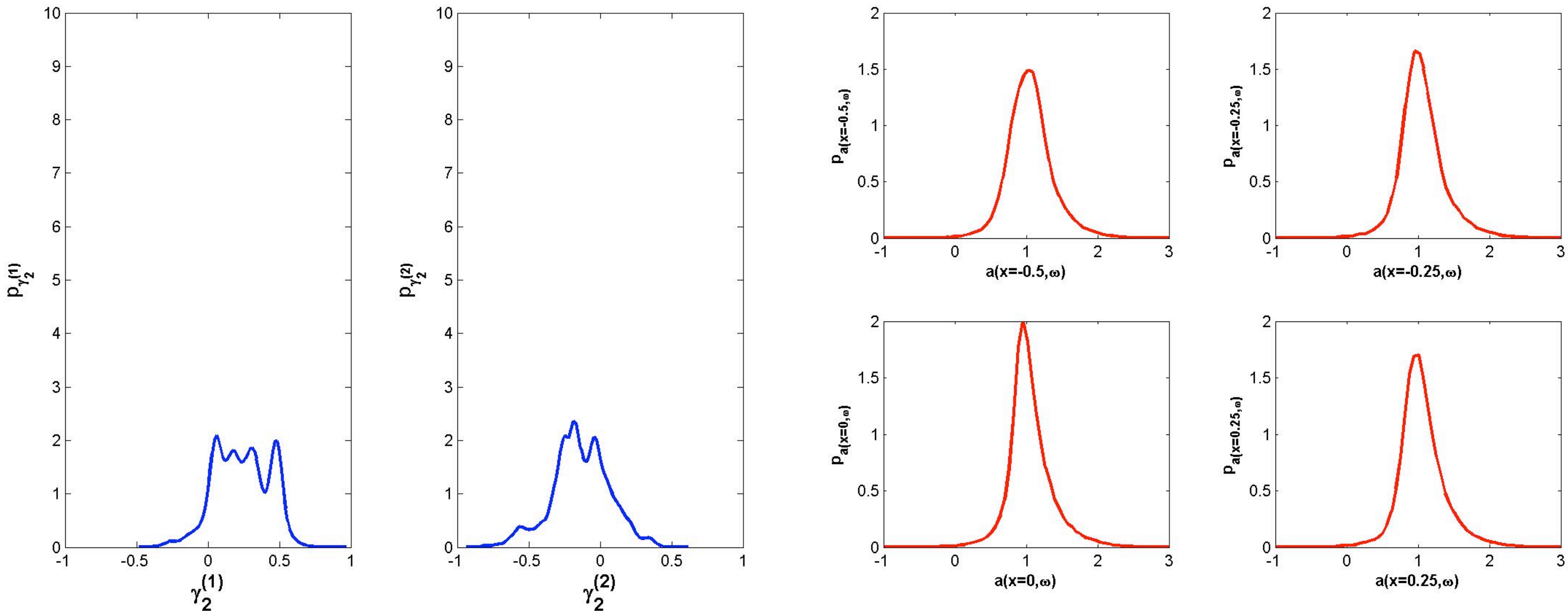

Representation of uncertainty: Bayesian inference

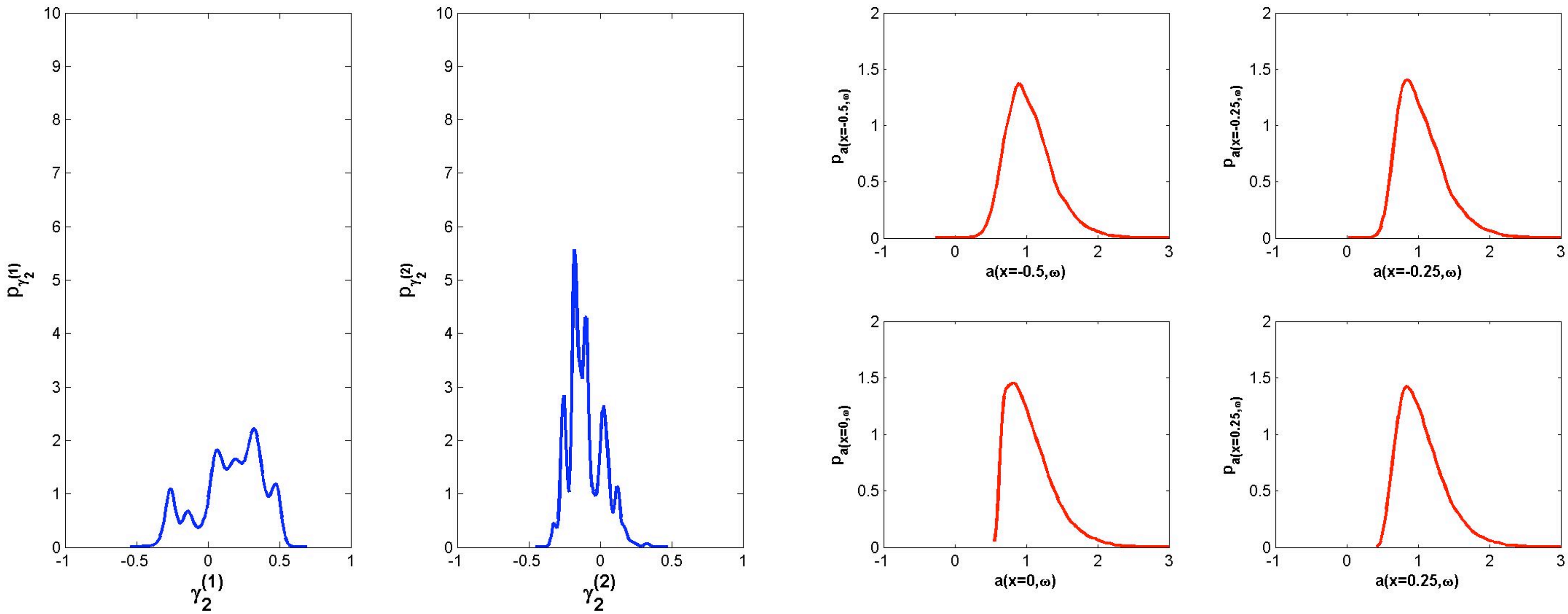

Representation of uncertainty: Bayesian inference

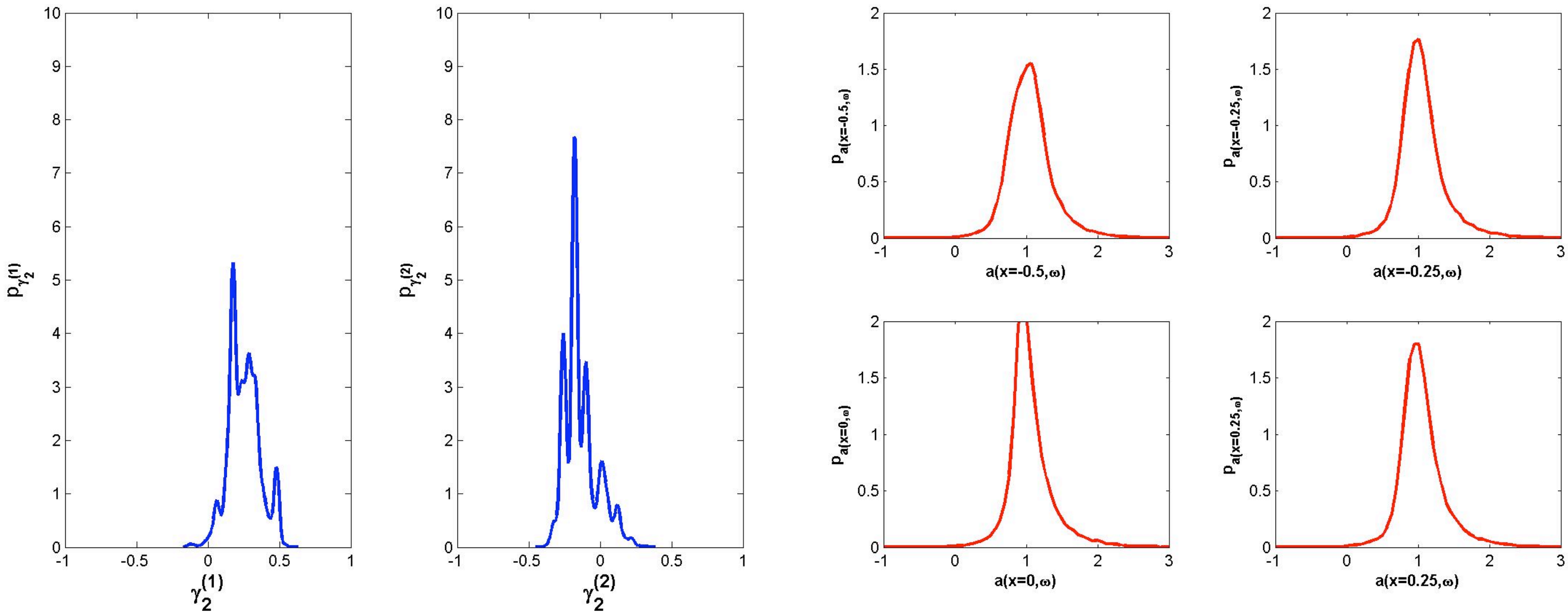

Representation of uncertainty: Bayesian inference

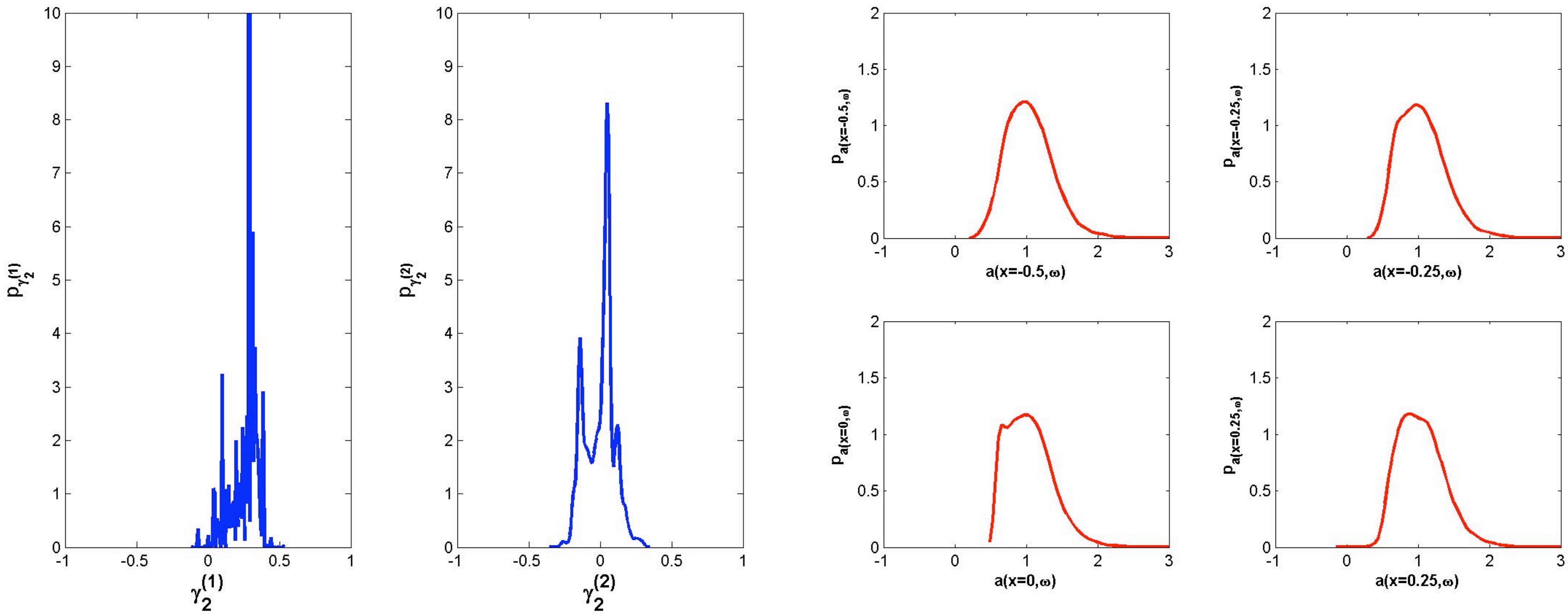

Representation of uncertainty: Bayesian inference

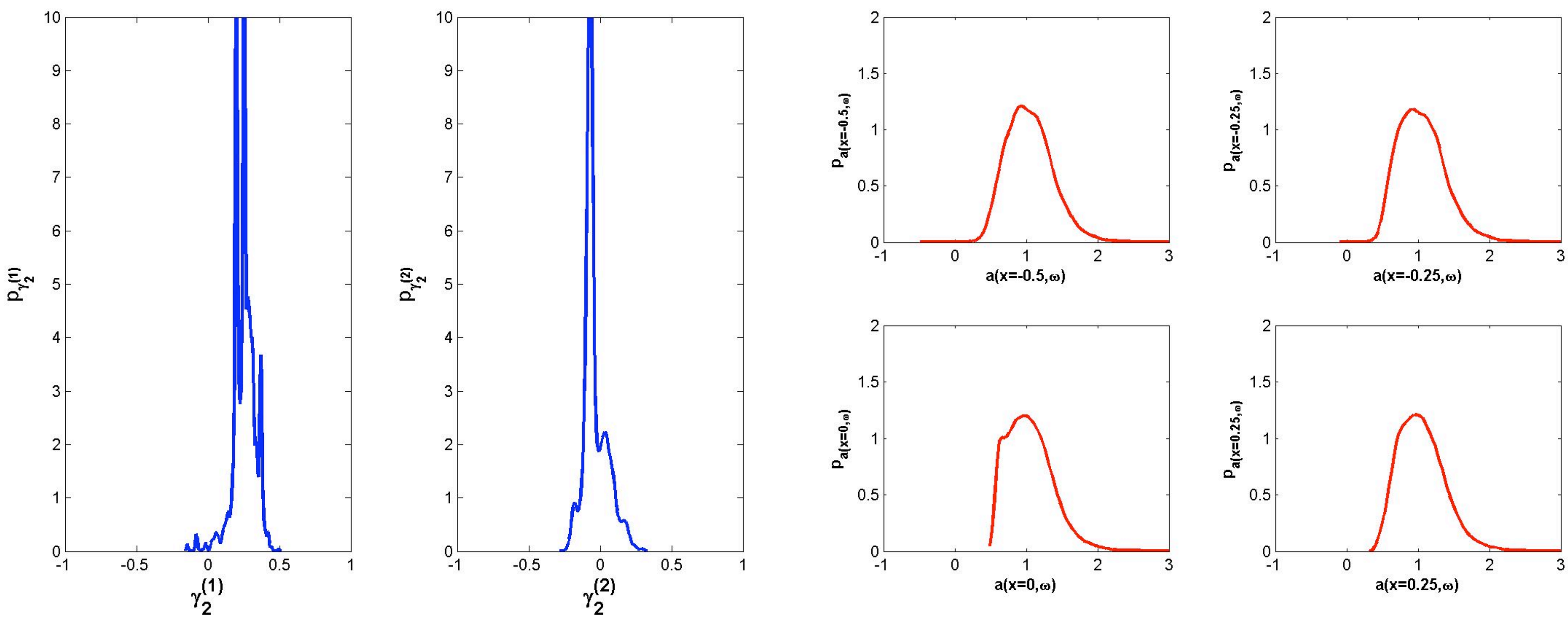

Representation of uncertainty: Bayesian inference

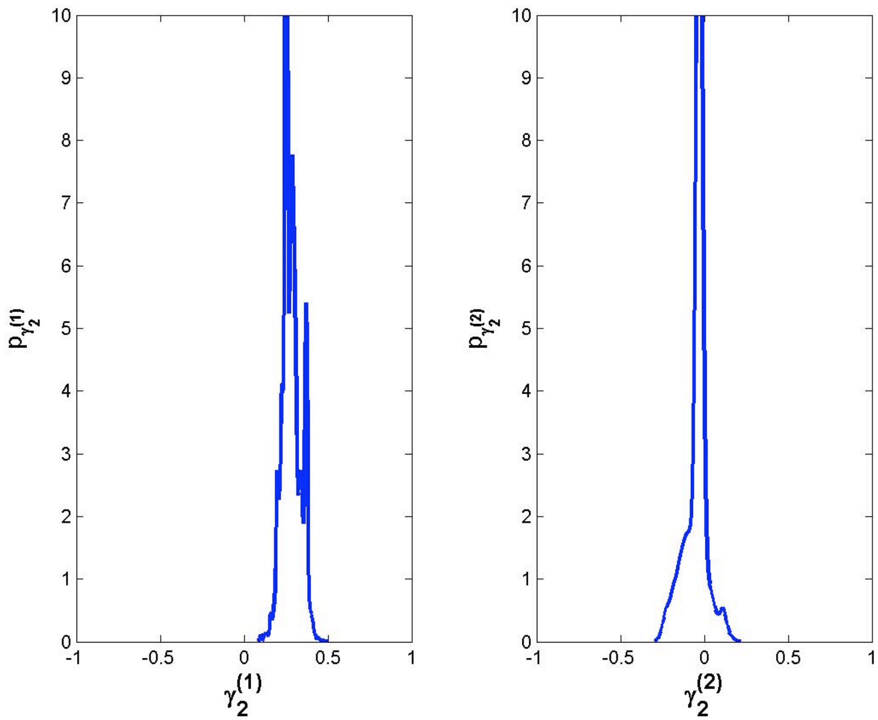

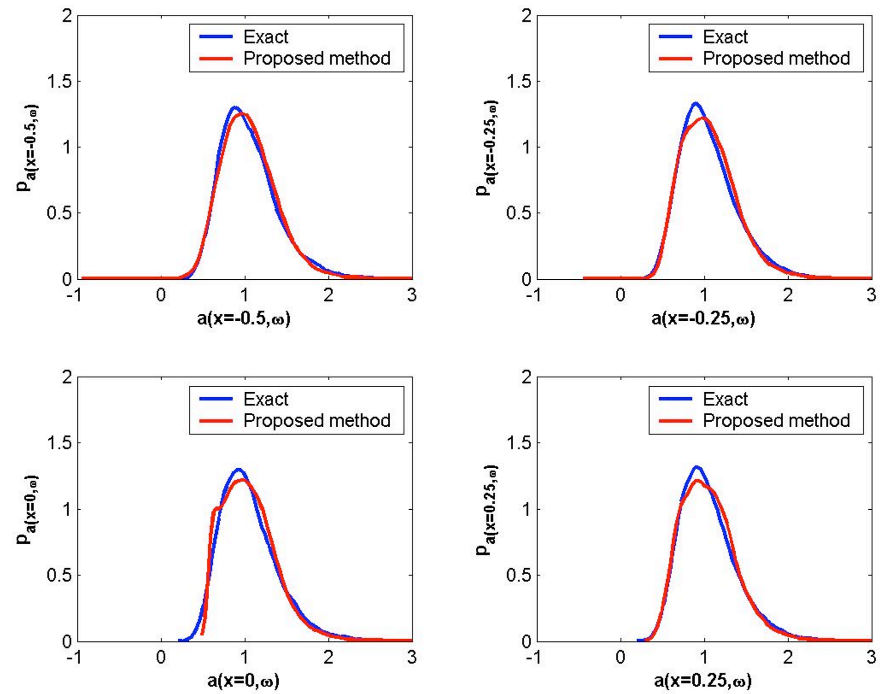

Representation of uncertainty: MaxEnt and Fisher information

Observe at N locations and n sets of observations.

Reduce dimensionality using KL.

Moments of observations as constraints:

$$\hat{\beta}_j = \frac{1}{n}\sum_{k=1}^{n}\left[\prod_{i=1}^{N}\left(z_i^{(k)}\right)^{m_{ij}}\right], \; j = 1,\cdots,p.$$

Maximum Entropy Density Estimation (MEDE) results in joint measure of KL variables:

$$p_{\mathcal{Z}}(\mathcal{Z}) = \exp\left[-\lambda^T T(\mathcal{Z}) - \xi(\lambda)\right]$$

$$T(z_1,\cdots,z_M) = \left[t_1(\mathcal{Z}),\cdots,t_p(\mathcal{Z})\right]^T$$

$$t_j(\mathcal{Z}) = \left(\prod_{i=1}^{M} z_i^{m_{ij}}\right), \quad j = 1,\cdots,p$$

Fisher Information Matrix:

$$\mathbf{F}_n(\lambda) = -E\left[\frac{\partial^2 \ln \ell(\lambda|\mathbf{Z}_n)}{\partial\lambda\partial\lambda^T}\middle|\lambda\right] \qquad \mathbf{Z}_n = \left[\mathcal{Z}_1^T,\cdots,\mathcal{Z}_n^T\right]^T$$

Then asymptotically (h denotes coefficients in polynomial chaos description of observations):

$$\mathbf{h}_q(\hat{\lambda}) \overset{\text{approx.}}{\sim} N(\mathbf{h}_q(\lambda), \mathbf{h}_q^{'}(\lambda)^T \mathbf{F}_n(\lambda)^{-1}\mathbf{h}_q^{'}(\lambda)), \; q = 1,\cdots,N$$

Stochastic FEM

$$\varepsilon_{p,h} = u\big|_d - \sum_{i=0}^{p} u_i \psi_i$$

Stochastic FEM

Variational Formulation:

Find $u \in H$ s.t.: $\mathcal{B}(u,v) = \mathcal{L}(v), \quad \forall v \in H$

Where:

$$H = H_0^1(D) \otimes L_2(\Gamma)$$

$$\Gamma \equiv \Gamma_1 \times \cdots \times \Gamma_M, \qquad \xi_i : \Omega \rightarrow \Gamma_i \subset \mathbb{R}$$

$$\mathcal{B}(v,w) \equiv \langle \textstyle\int_D a \nabla v . \nabla w dx \rangle, \quad \forall v, w \in H$$

$$\mathcal{L}(v) \equiv \langle \textstyle\int_D f v dx \rangle, \ \forall v \in H$$

Notice:

$\mathcal{B}(.,.)$ should be coercive and continuous

Stochastic FEM

Approximation Formulation:

Find $u_{X,Y} \in X \otimes Y$ .t.: $\mathcal{B}(u_{X,Y}, v) = \mathcal{L}(v), \quad \forall v \in X \otimes Y$

Where:

$$X \equiv X_h \subset H_0^1(D)$$

$$Y \equiv Y_p = \oplus_{i=1}^{p} \mathcal{P}_i \subset L_2(\Gamma)$$

$\mathcal{P}_i$ → i^{th} Homogeneous Chaos in $\{\xi_i(\theta)\}_{i=1}^{M}$

Write:

$$u_{X,Y}(x,\theta) = \sum_{i,j} u_{ij} N_i(x) \Psi_j(\theta) \xrightarrow{\;*\;} \mathcal{K}\mathcal{U} = \mathcal{F}$$

$N_i(x)$ → Basis in X

$\Psi_j(\theta)$ → Basis in Y

Typical System Matrix: 1st Order

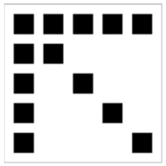

Typical System Matrix: 2nd Order

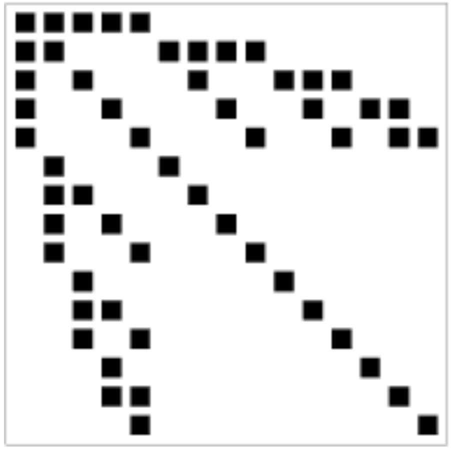

Typical System Matrix: 3rd Order

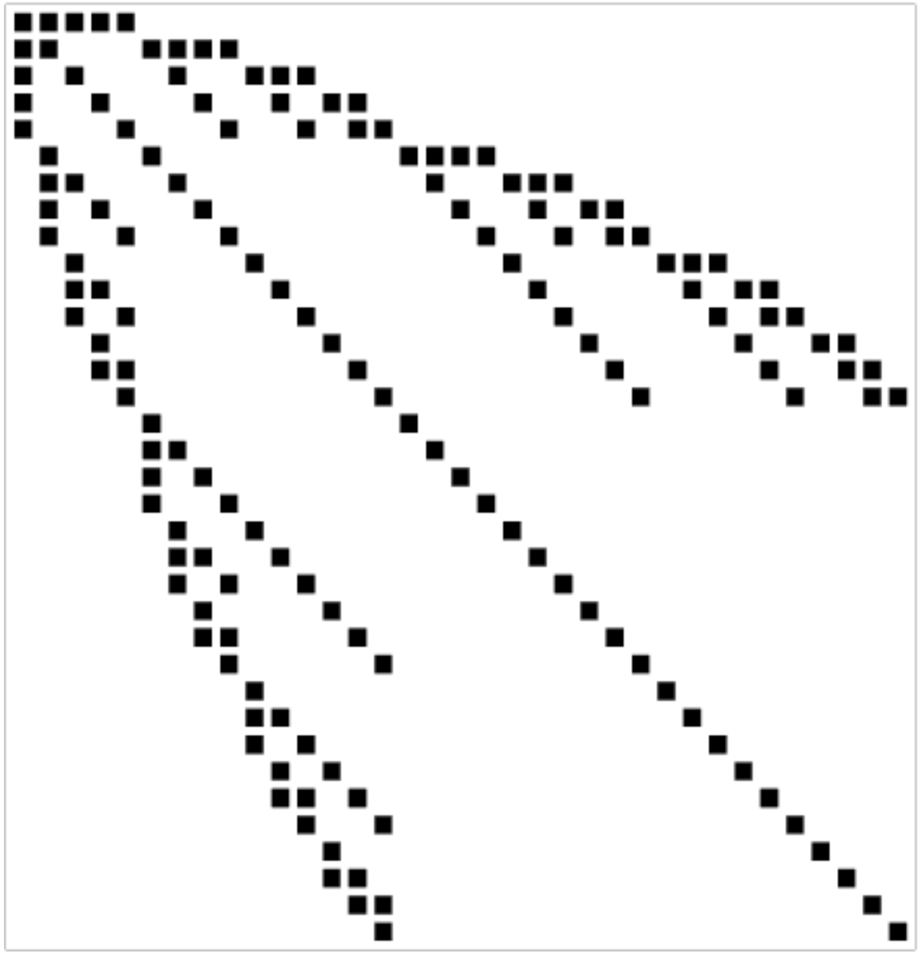

Efficient pre-conditioners

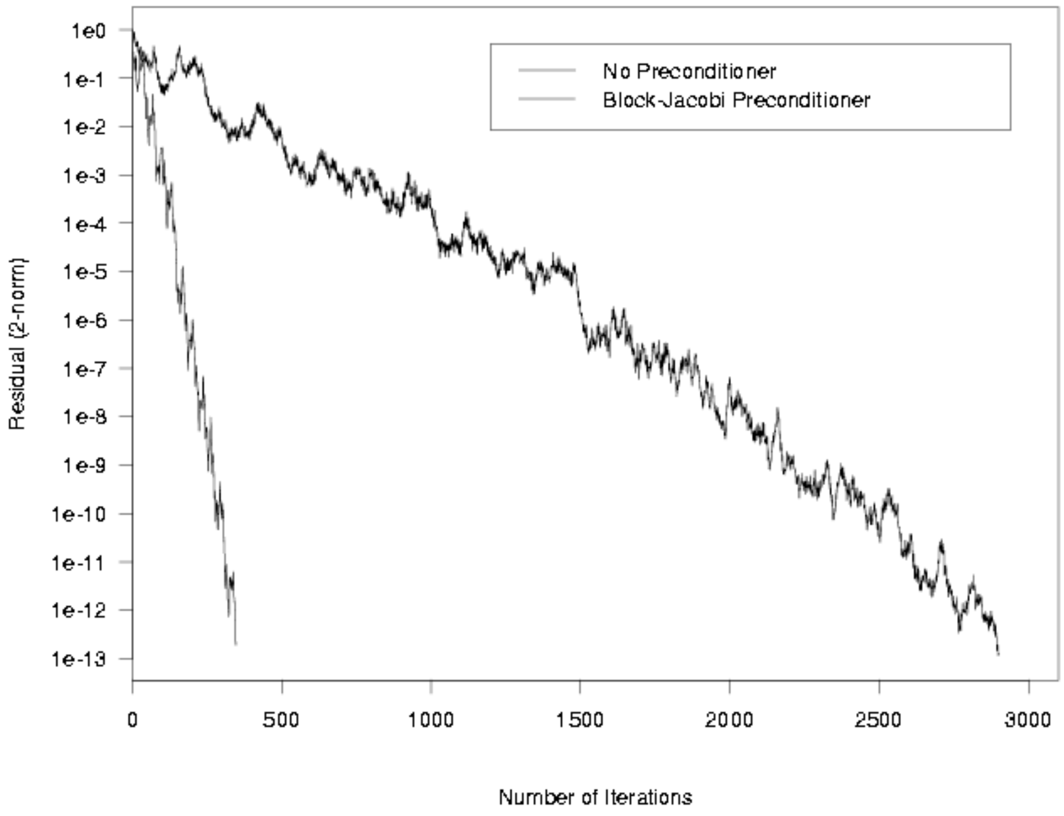

Stochastic FEM

Sources of Error:

- *Spatial Discretization Error:*

$$H_0^1 \to X$$

- *Random Dimension Discretization Error:*

$$L_2(\Gamma) \to Y$$

$$u_i(\theta) = \sum_{j=1}^{\infty} u_{ij} \Psi_j(\theta) \quad \to \quad u_i(\theta) = \sum_{j=1}^{P} u_{ij} \Psi_j(\theta)$$

- ❑ Joint error estimation is possible, for general measures, using nested approximating spaces (e.g. hierarchical FEM) (Doostan and Ghanem, 2004, 2005)

- ❑ Joint error estimation is possible, for special cases:
  - ❑ infinite-dimesional gaussian measure: Benth et.al, 1998
  - ❑ tensorized uniform measure: Babuska et.al, 2004

Using Components of Existing Analysis Software

$$\sum_{j=0}^{P} \left(\sum_{i} c_{ijk} \mathbf{K}_i \right) \mathbf{u}_j = \mathrm{f}_k, \quad k = 0, \ldots, P$$

$$\sum_{j=0}^{P} \mathbf{K}_{jk} \mathbf{u}_j = \mathrm{f}_k, \quad k = 0, \ldots, P$$

$$\mathbf{K}_0 \mathbf{u}_k = \mathrm{f}_k - \sum_{j \neq k} \sum_{i} c_{ijk} \mathbf{K}_{jk} \mathbf{u}_j - \sum_{j=0}^{P} (1 - \delta_{j0}) \mathbf{K}_{jk} \mathbf{u}_j$$

Essentially preconditioning with $\mathbf{K}_0$.

Only one deterministic solve required.   Minimal change to existing codes.

Need iterative solutions with multiple right hand sides.

Integrated into ABAQUS (not commercially).

Non-intrusive implementation

The solution $\mathbf{u}$ is a function of the basic random variables $\mathbf{x}_i$:

$$\mathbf{u} = f(\mathbf{x}_1, \ldots, \mathbf{x}_n)$$

where $f(....)$ is a mapping available through an analysis code.

A Polynomial Chaos Decomposition of the solution has the form:

$$\mathbf{u} = \sum_i \psi_i \mathbf{u}_i \qquad \mathbf{u}_i = \frac{\langle \mathbf{u}\psi_i \rangle}{||\psi_i||^2}$$

where the mathematical expectation is evaluated through a statistical average over a finite number of samples.

Error Estimator:

$$E = \frac{1}{n_s} \sum_{k=1}^{n_s} ||\boldsymbol{u}(a_k) - \boldsymbol{u}^{r,n_s}(a_k)||_{\mathbb{C}}^2$$

Example: Protein Labeling

Continuity and momentum equations:

$$\nabla \cdot u = 0$$

$$\frac{\partial u}{\partial t} + u \cdot \nabla u = -\nabla p + \nu \nabla^2 u$$

Wall electrostatic forces (Helmholtz-Smoluchowski relationship):

$$u_w = -\frac{\varepsilon \zeta}{\mu} \nabla_t \phi_w$$

Species concentrations:

$$\frac{\partial c_i}{\partial t} + \nabla \cdot [c_i (u + u_i^e)] = \nabla \cdot (D_i \nabla c_i) + \hat{w}_i$$

Electromigration velocity: $u_i^e = -\beta_i z_i F \nabla \phi$

Diffusivity: $D_i = RT\beta_i$

Electrostatic Field Strength:

$$\nabla \cdot (\sigma \nabla \phi) = -F \sum_i z_i \nabla \cdot (D_i \nabla c_i)$$

$$\sigma = F^2 \sum_i z_i^2 \beta_i c_i$$

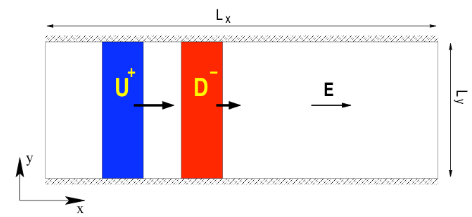

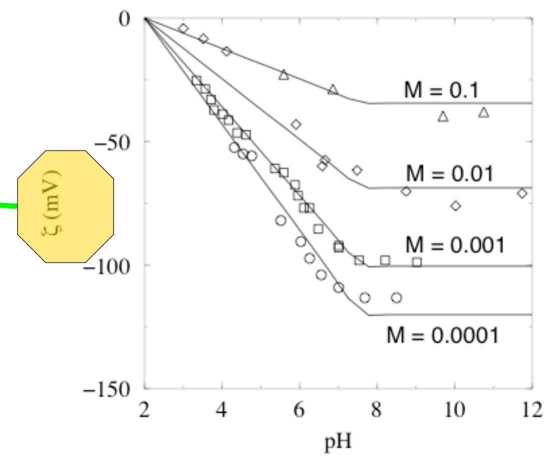

$$\zeta = \left\{ -(pH-2) + \left(\frac{1}{2} + \frac{1}{2}\tanh(5(pH-7.5))\right)(pH-7.6) \right\} \times \left(-2.7\ln(M + 2.3 \times 10^{-4})\right)$$

Protein Labeling: Stochastic Representations

Chaos representations of various stochastic parameters and solutions:

$$D(\xi) = \sum_{k=0}^{P} D_k \Psi_k(\xi) \qquad D_k = \frac{<\Psi_k D>}{<\Psi_k^2>}$$

$$u(x,t;\theta) = \sum_{k=0}^{P} u_k(x,t)\Psi_k(\theta)$$

$$c(x,t;\theta) = \sum_{k=0}^{P} c_k(x,t)\Psi_k(\theta)$$

$$\phi(x,t;\theta) = \sum_{k=0}^{P} \phi_k(x,t)\Psi_k(\theta)$$

$$\Psi_0 = 1,\ \Psi_1 = \xi,\ \Psi_2 = \xi^2 - 1,\ \Psi_3 = \xi^3 - 3\xi,\ \ldots$$

Equations governing evolution of Chaos coordinates:

$$\frac{\partial u_k}{\partial t} + \sum_{i=0}^{P}\sum_{j=0}^{P} C_{ijk}(u_i \cdot \nabla)\, u_j = -\nabla p_k + \sum_{i=0}^{P}\sum_{j=0}^{P} C_{ijk} \nu_i \nabla^2 u_j \qquad \forall k \qquad C_{ijk} = \frac{<\psi_i \psi_j \psi_k>}{<\psi_k^2>}$$

$$\frac{\partial c_{m,k}}{\partial t} + \sum_{i=0}^{P}\sum_{j=0}^{P} C_{ijk} \nabla \cdot \left(c_{m,i}(u_j + u^e_{m,j})\right) = \sum_{i=0}^{P}\sum_{j=0}^{P} C_{ijk} \nabla \cdot (D_{m,i} \nabla c_{m,j}) + \hat{w}_{m,k} \qquad \forall k$$

$$\sum_{i=0}^{P}\sum_{j=0}^{P} C_{ijk} \nabla \cdot (\sigma_i \nabla \phi_j) = -F \sum_m z_m \sum_{i=0}^{P}\sum_{j=0}^{P} C_{ijk} \nabla \cdot (D_{m,i} \nabla c_{m,j}) \qquad \forall k$$

$$\sigma_i = F^2 \sum_m z_m^2 \sum_{j=0}^{P}\sum_{k=0}^{P} C_{jki} \beta_{m,j} c_{m,k}$$

Implementation issues:

- ✓Stochastic toolkit (working on version 2)
- ✓Adapted time integration
- ✓Adapted spatial discretization

Protein Labeling: some results

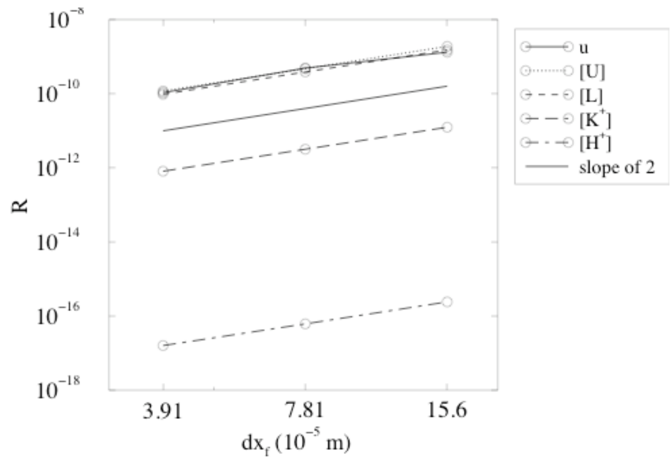

L2 norm of the difference between solutions on successive grids as a function of the fine grid spacing dxf. The slope of the lines shows a second-order spatial convergence rate for various species concentrations as well as the streamwise velocity.

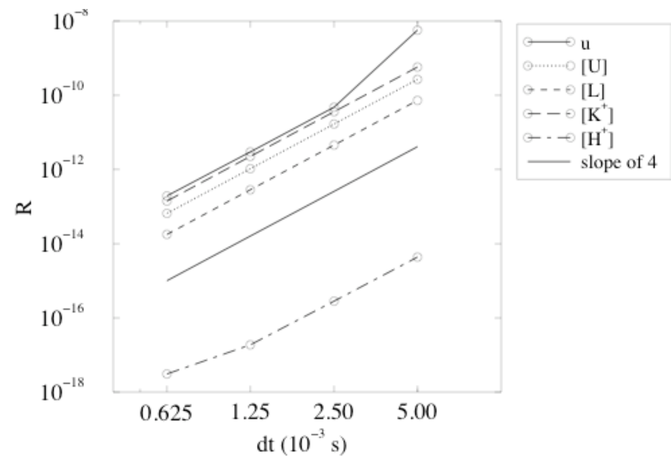

L2 norm of the difference between solutions at successive time steps as a function of the shorter time step dt. The slope of the lines shows a fourth-order temporal convergence rate for various species concentrations as well as the streamwise velocity.

Protein Labeling: some results

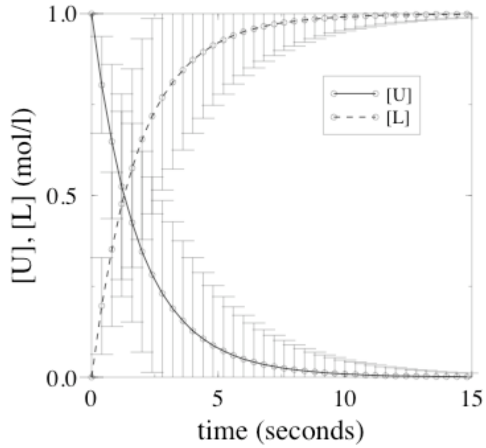

Time evolution of U and L concentrations in a homogeneous protein labeling reaction. The uncertainty in these concentrations, due to a 1% uncertainty in the labeling reaction rate parameters, is indicated by 63s ''error bars.''

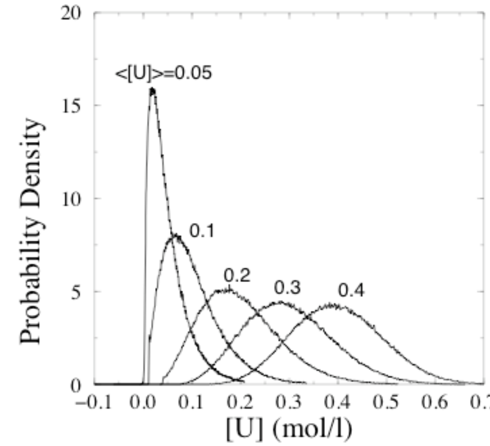

PDF of the unlabeled protein concentration at different mean values. As the unlabeled protein reacts away, its PDF becomes narrower and more skewed.

Major contributions of individual input parameters to the overall standard deviation in [L] in the area around the reaction zone at t=0.12 s, y=0.5 mm. The uncertainty in the applied voltage potential ''DV'' has the most dominant contribution to the overall standard deviation in [L].

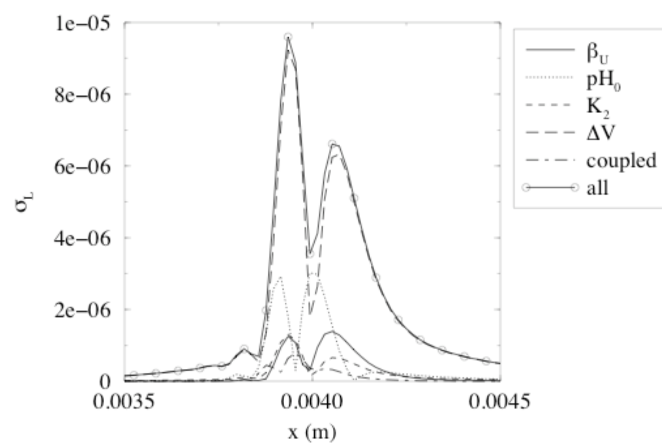

Protein Labeling: some results

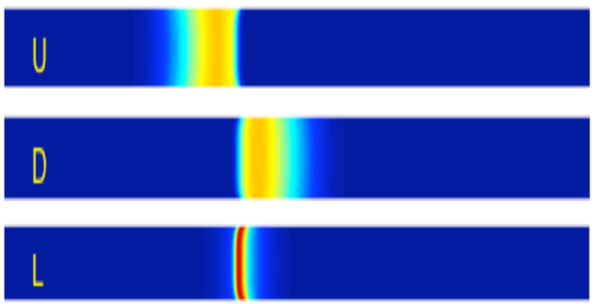

Mean concentrations of proteins U, L, and dye D at t=0.12 s. U and D just met and L is produced at their interface. The values of the contour levels go linearly from 0 (blue) to 1.3e-4 (red) mol/l

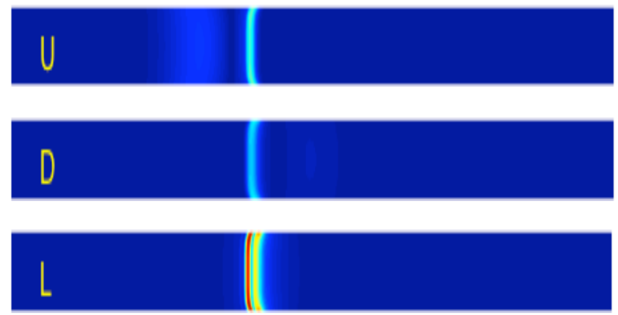

Standard deviation of the protein and dye concentrations at t=0.12 s. The values of the contour levels go linearly from 0 (blue) to 1.1e-5 mol/l (red). The largest uncertainties are found in the reaction zone.

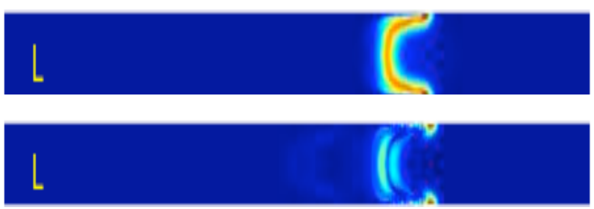

Mean (top) and standard deviation (bottom) of the labeled protein concentration L at t=0.50 s. The initially flat profiles are now severely distorted. The values of the contour levels go linearly from 0 (blue) to 3.2e-4 mol/l (red) in the top plot and from 0 (blue) to 1e-4 mol/l (red) in the bottom plot.

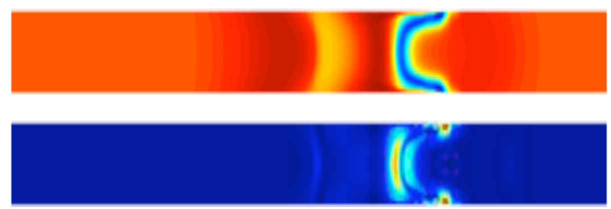

Mean (top) and standard deviation (bottom) of the electrical conductivity of the electrolyte solution at t=0.50 s. Annihilation of ions in the labeling reaction results in a significantly lower mean electrical conductivity near the L plug. The values of the contour levels go linearly from 7.1e-3 S/m(blue) to 1.3e-2 S/m(red) in the top plot and from 0 (blue) to 1.5e-3 S/m (red) in the bottom plot.

Protein Labeling: some results

Mean (top) and standard deviation (bottom) of the electrical field strength in the x direction at t=0.50 s. Near the L plug, the mean streamwise electrical field strength is about 40% higher than in the undisturbed flow. The values of the contour levels go linearly from 91.4 kV/m (blue) to 146 kV/m (red) in the top plot and from 0.20 kV/m (blue) to 13 kV/m (red)in the bottom plot.

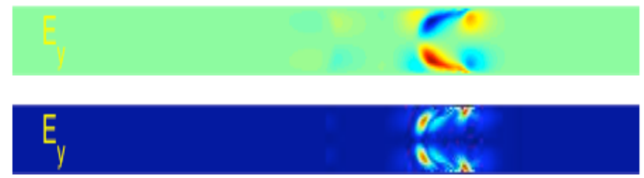

Mean (top) and standard deviation (bottom) of the electrical field strength in the y direction at t=0.50 s. The magnitude of the mean of this field strength is up to 15% of the initial field strength in the x direction. The values of the contour levels go linearly from 216.3 kV/m (blue) to 16.3 kV/m (red) in the top plot and from 0 (blue) to 5.8 kV/m (red) in the bottom plot.

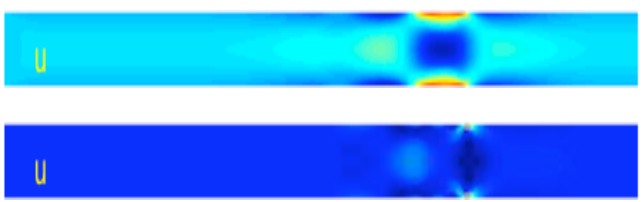

Mean (top) and standard deviation (bottom) of the streamwise velocity at t=0.50 s. The local increase in the electroosmotic wall velocity leads to recirculation zones near the L plug. The largest uncertainties are found near the wall. The values of the contour levels go linearly from 6.8 mm/s (blue) to 9.1 mm/s (red) in the top plot and from 5.6e-3 mm/s (blue) to 0.59 mm/s (red) in the bottom plot.

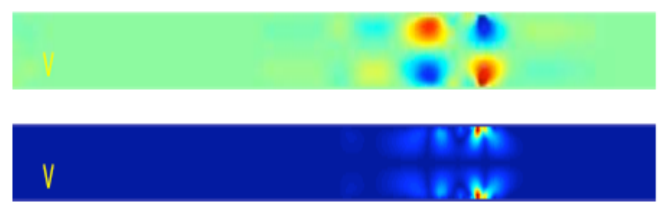

Mean (top) and standard deviation (bottom) of the wallnormal velocity at t=0.50 s. The mean of this velocity has a magnitude of up to 6 % of the initial streamwise velocity. The values of the contour levels go linearly from 20.56 mm/s (blue) to 0.56 mm/s (red) in the top plot and from 0 (blue) to 0.26 mm/s (red) in the bottom plot.

Connection to multiscale analysis

Need innovative uni-scale models that know what to do with other-scale information: (eg. stochastic homogenization; stochastic equation-free; multiscale mechanics)
(reference: Jardak, M. and Ghanem, R. in CMAME)

New stochastic models for processes exhibiting variation over a few scales. Where spectral analysis, correlation analysis does not apply
(reference: Jianxu S., PhD thesis at Hopkins)

Multiscale data assimilation: transform coarse scale measurements into fine scale parameters (both deterministic and stochastic)
(reference: Zou, Y. and Ghanem, R. in SIAM MMS)

Need logic for targeted scale adaptation: signatures of various subscales in stochastic representation at coarse scale.

On the horizon

- **C**ritical examination of probabilistic **models** of data:
  - Physical and mathematical implications of these models.
  - Connection to multi-scale properties of materials and systems.
  - Adapted bases for enhanced convergence.
- **E**fficient **numerical** solvers:
  - Using existing codes.
  - Very high-dimensional quadrature.
  - Intrusive algorithms.
- **Visualization** of probabilistic information as decision aids.
- **Model reductions** that maximize information content.
- **Optimization** under uncertainty: uncertainty in objective function, decision variables, and constraints.
- **Validation** of complex interacting systems.
- **Error estimation** and refinement: allocation of resources to physical and numerical experiments.
- **Fusion** of experiments and model-based predictions.

Selected references

Ghanem, R. and Doostan, A., ``On the Construction and Analysis of Stochastic Predictive Models: Characterization and Propagation of the Errors Associated with Limited Data,'' submitted to Journal of Computational Physics, 2005.

Descelliers, C., Ghanem, R. and Soize, C. ``Maximum likelihood estimation of stochastic chaos representation from experimental data,'' to appear in International Journal for Numerical Methods in Engineering.

Reagan MT, Najm HN, Pebay PP, Knio, O. and Ghanem, R., ``Quantifying uncertainty in chemical systems modeling,'' International Journal of Chemical Kinetics, Vol. 37, No. 6, pp. 368-382, 2005.

Le Maitre,O., Reagan, M.T., Debusschere, B., Najm, H.N., Ghanem, H.N. and Knio, O., ``Natural convection in a closed cavity under stochastic, non-Boussinesq conditions,'' SIAM Journal of Scientific Computing, Vol. 26, No. 2, pp. 375-394, 2004.

Soize, C., and Ghanem, R. ``Physical Systems with Random Uncertainties: Chaos representations with arbitrary probability measure,'' SIAM Journal of Scientific Computing, Vol. 26, No. 2, pp. 395-410, 2004.

Debusschere, B., and Najm, H.N., Matta, A., Knio, O., Ghanem, R., and LeMaitre, O., " Protein labeling reactions in electrochemical microchanel flow: Numerical simulation and uncertainty propagation,'' Physics of Fluids, Vol. 15, No. 8, pp. 2238-3350,2003.

Pellissetti, M. and Ghanem, R., ``A method for the validation of predictive computations using a stochastic approach,'' ASME Journal of Offshore Mechanics and Arctic Engineering, Vol.126, No. 3, pp. 227-234, 2004.

Le Maitre, O.P., Najm, H., Ghanem, R. and Knio, O., ``Multi-resolution analysis of Wiener-type uncertainty propagation schemes,'' Journal of Computational Physics, Vol 197, No. 2, pp 502-531, 2004.

Le Maitre, O., Reagan, M., Najm, H., Ghanem, R., and Knio, O., ``A stochastic projection method for fluid flow. II: Random Process,'' Journal of Computational Physics, Vol. 181, pp. 9-44, 2002.

Sarkar, A. and Ghanem, R., ``A substructure approach for the mid-frequency vibration of stochastic systems,'' JASA, Vol. 113, No. 4, pp. 1922-1934, 2003.

Ghanem, R., and Red-Horse, J., ``Propagation of uncertainty in complex physical systems using a stochastic finite element approach,'' Physica D, Vol. 133, No. 1-4, pp. 137-144, 1999.

Ghanem, R., and Dham, S., ``Stochastic finite element analysis for multiphase flow in heterogeneous porous media,'' Transport in Porous Media, Vol. 32, pp. 239-262, 1998.

Ghanem, R., ``Scales of fluctuation and the propagation of uncertainty in random porous media,'' Water Resources Research, Vol. 34, No. 9, pp. 2123-2136, September 1998.

Ghanem, R., and Spanos, P., Stochastic Finite Elements: A Spectral Approach, Springer Verlag, 1991. (reissued by Dover Publications, 2003.)